

## Review Commentary

# Functional aspects of ribosomal architecture: symmetry, chirality and regulation<sup>†‡</sup>

Raz Zarivach,<sup>1</sup> Anat Bashan,<sup>1</sup> Rita Berisio,<sup>2,†</sup> Joerg Harms,<sup>2</sup> Tamar Auerbach,<sup>1,2</sup> Frank Schluenzen,<sup>2</sup> Heike Bartels,<sup>2</sup> David Baram,<sup>1,2</sup> Erez Pyetan,<sup>1,2</sup> Assa Sittner,<sup>1</sup> Maya Amit,<sup>1</sup> Harly A. S. Hansen,<sup>2</sup> Maggie Kessler,<sup>1</sup> Christa Liebe,<sup>2</sup> Anja Wolff,<sup>2</sup> Ilana Agmon<sup>1</sup> and Ada Yonath<sup>1,2\*</sup>

<sup>1</sup>Department of Structural Biology, The Weizmann Institute, 76100 Rehovot, Israel

<sup>2</sup>Max-Planck-Research Unit for Ribosomal Structure, 22603 Hamburg, Germany

Received 16 November 2003; revised 12 March 2004; accepted 17 March 2004

**ABSTRACT:** High-resolution structures of both ribosomal subunits revealed that most stages of protein biosynthesis, including decoding of genetic information, are navigated and controlled by the elaborate ribosomal architectural design. Remote interactions govern accurate substrate alignment within a flexible active-site pocket [peptidyl transferase center (PTC)], and spatial considerations, due mainly to a universal mobile nucleotide, U2585, ensure proper chirality by interfering with D-amino-acids incorporation. tRNA translocation involves two correlated motions: overall mRNA/tRNA (messenger and transfer RNA) shift, and a rotation of the tRNA single-stranded aminoacylated-3' end around the bond connecting it with the tRNA helical-regions. This bond coincides with an axis passing through a sizable symmetry-related region, identified around the PTC in all large-subunit crystal structures. Propelled by a bulged universal nucleotide, A2602, positioned at the two-fold symmetry axis, and guided by a ribosomal-RNA scaffold along an exact pattern, the rotatory motion results in stereochemistry optimal for peptide-bond formation and in geometry ensuring nascent proteins entrance into their exit tunnel. Hence, confirming that ribosomes contribute positional rather than chemical catalysis, and that peptide bond formation is concurrent with A- to P-site tRNA passage. Connecting between the PTC, the decoding center, the tRNA entrance and exit points, the symmetry-related region can transfer intra-ribosomal signals between remote functional locations, guaranteeing smooth processivity of amino acids polymerization. Ribosomal proteins are involved in accurate substrate placement (L16), discrimination and signal transmission (L22) and protein biosynthesis regulation (CTC). Residing on the exit tunnel walls near its entrance, and stretching to its opening, protein-L22 can mediate ribosome response to cellular regulatory signals, since it can swing across the tunnel, causing gating and elongation arrest. Each of the protein CTC domains has a defined task. The N-terminal domain stabilizes the intersubunit-bridge confining the A-site-tRNA entrance. The middle domain protects the bridge conformation at elevated temperatures. The C-terminal domain can undergo substantial conformational rearrangements upon substrate binding, indicating CTC participation in biosynthesis-control under stressful conditions. Copyright © 2004 John Wiley & Sons, Ltd.

**KEYWORDS:** ribosomes; peptide-bond formation; positional-catalysis; D-amino acids; tunnel dynamics; elongation arrest; protein CTC; protein L22

## INTRODUCTION

Ribosomes are universal cellular riboprotein assemblies that catalyze the translation of the genetic code into

proteins. This process, known as protein biosynthesis, involves the expression of the genetic instructions, encoded on the genomic DNA in the form of polynucleotides, into protein, namely polyamino acids. Accordingly, ribosomes act as polymerases that not only form peptide bonds, but also ensure the elongation of the nascent protein chains. Ribosomes from all living cells consist of two subunits of unequal size, which associate upon the initiation of protein biosynthesis and dissociate once this process is terminated. Each ribosomal subunit has a defined composition, but the exact number of its components relates to the ribosomal source. A typical prokaryotic large ribosomal subunit, called 50S, has a molecular weight of  $1.5 \times 10^6$  Da and contains about 35 proteins (designated L1, L2, etc.) and two RNA chains (23S RNA

\*Correspondence to: A. Yonath, Department of Structural Biology, The Weizmann Institute, 76100 Rehovot, Israel.

E-mail: ada.yonath@weizmann.ac.il

<sup>†</sup>Permanent address: Institute of Biostructure and Bioimaging, CNR, 80138 Napoli, Italy.

<sup>‡</sup>Paper presented at the 9th European Symposium on Organic Reactivity, 12–17 July 2003, Oslo, Norway.

Contract/grant sponsor: US National Institute of Health; Contract grant number: GM34360.

Contract/grant sponsor: German Ministry for Science and Technology; Contract/grant number: BMBF05-641EA.

Contract/grant sponsor: Kimmelman Center for Macromolecular Assemblies.

and 5S RNA, consistent with their size) with a total of  $\approx 3000$  nucleotides. The small prokaryotic ribosomal subunit, 30S, has a molecular weight of  $8.5 \times 10^5$  Da and contains one RNA chain (16S) of over 1500 nucleotides and  $\approx 20$  proteins (designated S1, S2, etc.).

Each of the ribosomal subunits has well defined tasks. The small ribosomal subunit facilitates the initiation of the translation process, and is involved in choosing the frame to be translated, in decoding the genetic message, and in controlling the fidelity of codon–anticodon interactions. The large ribosomal subunit forms the peptide bond and is responsible for channeling the nascent proteins through their exit tunnel. As protein biosynthesis is performed through a cooperative effort by both subunits, and as cell vitality requires an efficient process of protein formation, the ribosome possesses features allowing transmission of signals between its various functional sites. Furthermore, evidence is being accumulated for ribosomal involvement in regulatory and control mechanisms, all requiring fast response of specific ribosomal components.

The genetic instructions, encoded in the DNA, are brought to the ribosome by messenger-RNA (mRNA), which is basically an RNA duplicate of a segment of the genomic DNA. Aminoacylated transfer-RNA (tRNA) molecules deliver the amino acids to the ribosome. These are large L-shaped molecules, and although they are built primarily of double helices, they exploit single stranded regions for their functions: decoding the genetic information and participating in peptide bond formation. The tRNA anticodon stem loop that interacts with the nucleotide triplet to be decoded via base pairing with the mRNA, binds to the small subunit. Located over 70 Å away, the other end of the tRNA molecule, namely the universal tRNA 3' end that is built of the three nucleotides (CCA), binds the amino acid to be incorporated in the growing protein [Fig. 1(a)]. During protein biosynthesis, both of the amino acids to be incorporated in the nascent protein and the newly formed polypeptide chain bind covalently to this universal CCA moiety.

The ribosome possesses three tRNA binding sites, named according to their function. The A-site hosts the aminoacylated tRNA, the P-site is that of the peptidyl tRNA and the E-site designates the position of the existing free tRNA once a peptide bond has been formed. The elongation of the polypeptide chain is associated with  $A \rightarrow P \rightarrow E$  translocation of the mRNA together with the tRNA molecules bound to it. In each step of the elongation event, a new peptide bond is being formed by a nucleophilic attack of the aminoacyl-tRNA amine group on the peptidyl-tRNA carbonyl carbon. The leaving group of this reaction is a free tRNA molecule, which exits the ribosome through the E-site as a part of the overall mRNA–tRNA translocation. The entire cycle of elongation is extremely fast. Only about 50 ms are required to accomplish it, from the stage of tRNA selection by base pairing with the mRNA, until the leaving group, namely a free tRNA is released, and

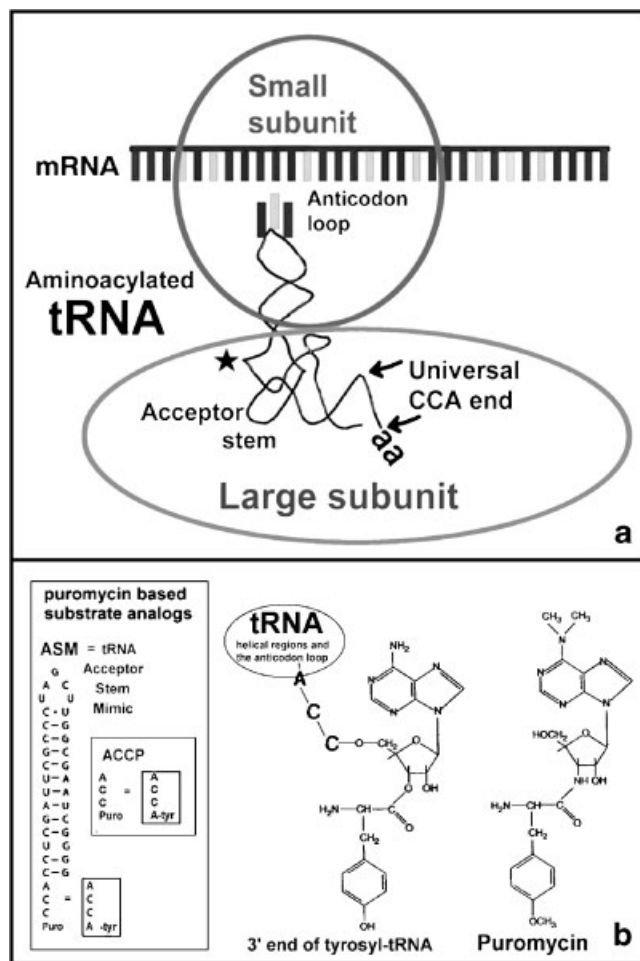


**Figure 1.** The tRNA molecule and its mimics. A schematic representation of the tRNA molecule, and its overall positioning within the active ribosome are shown in (a). The two functional single-stranded regions are highlighted. The star designates the approximate position of one of the ends of the tRNA acceptor stem, which stretches all the way to the CCA end. This star also shows the approximate position of the loop end of the ASM, (a 35 nucleotide chain mimicking the tRNA acceptor stem and its aminoacylated 3' end) the long tRNA mimic used by us, shown in the insert, which also contains a tRNA 3' end mimic, known as ACCP. Both mimics include a CCA end, based on the structure of puromycin, a universal ribosomal inhibitor. The similarity between aminoacylated tRNA 3' end and puromycin is shown in (b), which explains the high level of competition

peptide bond formation consumes a very small portion of this time.

Crystallography of ribosomes, initiated over two decades ago<sup>1</sup> recently yielded several three-dimensional structures of free and complexes ribosomal particles<sup>2–16</sup> and enabled the assignments of the three tRNA binding sites on each of the ribosomal subunits to be made [plate 1(a) and (b)]. They also confirmed the notion that the main parts of the A- and P-site tRNA molecules are roughly parallel to each other, whereas the E-site tRNA has to rotate while exiting the ribosome.<sup>6,7</sup> These structures revealed that the interface surfaces of both subunits are rich in RNA, and that for ribosomal proteins the

globular domains reside on the ribosomal surface exposed to the solution and send long tails or loops to the interior of the particles. The ribosomal RNA, which comprises about two thirds of the ribosomal mass, possess elaborate and intricate structural elements, most of which are stabilized by the extremely long termini or extended loops of the ribosomal proteins that penetrate into the RNA features.

Analysis of the structures of the ribosomal complexes with substrate analogues revealed unambiguously that both ribosomal active sites, namely the decoding center in the small subunit and the peptidyl transferase center (PTC) in the large subunit, consist exclusively of ribosomal RNA (rRNA): thus indicating that the ribosome is a ribozyme. The significance of the rRNA contributions to the biosynthetic process is substantiated by the modes of action of many antibiotics. These natural, semi-synthetic or man-made compounds are designed to interfere with bacterial metabolism by inhibiting fundamental cell processes. As a central element of the cell life cycle, the ribosome is one of the main targets for a broad range of antibiotics of a structurally diverse nature. Because of its huge size, the ribosome offers, theoretically, numerous different binding sites. Nevertheless, the crystal structures of more than a dozen complexes of antibiotics bound to the large subunit from *Deinococcus radiodurans*, a eubacterium proved to be suitable to serve as a pathogen model for ribosomal antibiotics, show that practically all of the known drugs utilize a single or very few binding sites.<sup>12–16</sup>

The findings presented in this review are based mainly on the high-resolution structures of the small ribosomal subunit from *Thermus thermophilus* T30S<sup>4</sup> [Plate 1(a)] and the large ribosomal subunit from *D. radiodurans*, D50S, in its free form<sup>7</sup> [Plate 1(b)] as well as in complexes with various mimics of aminoacylated tRNA molecules.<sup>8</sup> Here, we discuss some of the latest advances in the understanding of the molecular basis of the catalytic mechanism of peptide bond formation, and of the ribosomal action as an amino acid polymerase. We also analyze the ribosomal architecture and highlight selected ribosomal regulatory tasks.

## SPECTACULAR RIBOSOMAL ARCHITECTURE

### Global motions

Large-scale movements of ribosomal components, mRNA and the ribosomal substrates, the tRNA molecules, are essential for almost all stages of protein biosynthesis. Global movements of sizable ribosomal features were detected by cryo-electron microscopy during translocation of the mRNA/tRNA molecules, a process assisted by several non-ribosomal factors.<sup>17,18</sup> More accurate crystallographic investigations, exploiting comparative studies performed on the available high-resolution structures of the free and the complexes of ribosomal particles, also indicated motions in both subunits. The

mobile architecture of the small ribosomal subunit seems to be designed for its tasks in controlling the fidelity of the decoding process. The small subunit is built of several domains, radiating from a junction located near the decoding center [Plate 1(a)], indicating correlated internal mobility. The decoding center organizes the mRNA and the tRNA and provides the site for codon–anticodon interactions. A head-to-shoulder motion in the small subunit [Plate 1(a)] allows threading of the incoming mRNA through a dynamic pore, and the platform, located at the opposite side of the particle, is likely to perform the motions that facilitate the mRNA exit.<sup>4,19–21</sup> The pivotal point for this motion is probably the connection between the head and the main structural junction, in the vicinity of the binding site of spectinomycin, an antibiotic found to trap the small subunit at a particular conformation, thus disabling the head motions.<sup>22</sup> During elongation, the mRNA advances along a curved channel on the small subunit interface, and in order to ensure cognate tRNA selection at the A-site [Plate 1(a)], a specific conformation of the small subunit is required.<sup>22</sup>

Similarly, the two large subunit lateral protuberances, namely the L7/L12 stalk and the L1 arm [Plate 1(b)], were shown to possess dynamic properties and can undergo substantial conformational rearrangements.<sup>21</sup> By analyzing the available ribosomal high-resolution structures, a correlation between their structure and the functional state of the ribosome was revealed. Thus, they assume well defined, albeit dramatically different conformations in the complexed ribosome<sup>6</sup> compared with the unbound large ribosomal subunit,<sup>7</sup> They can readily become disordered [Plate 1(b)] when exposed to an environment which is very different from that leading to efficient protein biosynthesis, as seen in the crystal structure of the large subunit from *Haloarcula marismortui*, H50S.<sup>2</sup> The relative motions of these two features, which facilitate the A-site tRNA entrance (L7/L12 stalk) and the E-site tRNA exit (L1 arm), are probably associated with the motions of two features, located in the PTC vicinity, which were assigned as molecular switches. These are the multi-task inter-subunit bridge B2a [Plate 1(f)] that is likely to assist the A- to P-site tRNA acceptor-stem shift,<sup>11,21</sup> and the PTC nucleotide A2602 (*Escherichia coli* nomenclature is being used throughout) that seems to be involved in A- to P-translocation within the PTC.<sup>8,9,11</sup>

The PTC itself possesses the dynamic properties required for facilitating the correctly bound A-site tRNA to the P-site and for assisting rearrangements of less well aligned substrates.<sup>8,9,11,21</sup> It is located close to the subunit interface, at the bottom of a cavity in the large ribosomal subunit. The peripheral upper rim of this cavity includes a ribosomal protein, L16, but the PTC itself is formed exclusively by ribosomal RNA [Plate (1b–d)]. Striking nets of extensive interactions between the tRNA acceptor stem and the upper rim of the PTC cavity were observed in the structure of the whole ribosome from *T. thermophilus* complexed with three tRNAs<sup>6</sup> and

in complexes of tRNA acceptor-stem mimics with the large ribosomal subunit.<sup>8</sup> This finding stimulated analysis of several substrate analogue binding modes, which led to assessment of the relative significance of the parameters contributing to precise and productive tRNA placement. Substrate analogues, designed to mimic different portions of aminoacylated tRNA, were used for this analysis. These include compounds representing the CCA moiety, such as a tetra-nucleotide called ACCP (ACC–puromycin), to polynucleotides mimicking the entire portion of the tRNA that interacts with the large subunit, such as ASM, built of 35 nucleotides [Fig. 1(b) and Plate 1(c)]. The ends of all of these analogues contain puromycin, a universal ribosomal inhibitor whose structure mimics tyrosylated adenine [Fig. 1(b)].

The results of these studies indicate that the global localization of the tRNA molecules is based on the match between the overall ribosomal architecture and the size and shape of the tRNA molecules. Two universal base pairs between the 3' ends of both A- and P-site tRNAs and the ribosomal counterparts in the A-[Plate 1(c)] and P-sites (A-site G2553; P-site G2251), identified previously by biochemical methods,<sup>23</sup> govern the approximate heights of the fairly flexible single stranded tRNA 3' ends. The precise tRNA placement, however, is dominated by the interactions of the tRNA helical acceptor stem with the upper rim of the PTC cavity, remotely from the PTC lower end, where the peptide bond is being formed [Plate 1(c) and (d)].<sup>8,9,11</sup>

**Plate 1.** The two ribosomal subunits: structure, flexibility and functional dynamics. (a) and (b) The high resolution structures of the two eubacterial ribosomal subunits. RNA is shown in silver-gray. The main chains of the various proteins are shown as ribbons, colored arbitrarily. Selected functional relevant features are shown, with their traditional names. The approximate positions of the tRNA anticodon loops and the beginning of acceptor stems of the A-, P- and E-site tRNA are marked on the small and the large subunits, respectively. (a) The structure of the small ribosomal subunit, T30S<sup>4</sup>. P, the position of the P-site anticodon loop, also designates the decoding center. The red arrows designate the suggested head and platform motions involved in mRNA translocation. The left arrow describes the motion required for creating the mRNA entrance pore. (b) The structure of the large ribosomal subunit, D50S.<sup>7</sup> Red circles designate highly flexible functional relevant regions that can readily become disordered, as seen in H50S structure.<sup>2</sup> (c) and (d) show the positioning of ASM and ACCP, the two tRNA mimics described in Fig. 1(b), within the PTC pocket. The actual difference electron density maps and the position of the universal base pair that governs A-site relative height are shown in (c). (d) The PTC pocket, including the docked A- and P-site tRNAs (ribbon representation in cyan and olive-green, respectively) and ASM (atoms in red). This view highlights the contributions of H69 and protein L16 to the precise positioning of ASM. The RNA components of the PTC pocket are numbered and colored differently. Note that almost all features of the PTC belong to the region highlighted in blue. (e) and (f) Protein L16 and bridge B2a [the tip of H69, as given in (d)], two key components of the periphery of the upper rim of the PTC pocket, which contribute to the remote positioning of the tRNA substrates. (e) Indicates the fold similarity between the eukaryotic<sup>7</sup> (DL16) and archaeon (HL10e)<sup>2</sup> protein. (f) Shows the conformations of bridge B2a (H69) in the 5.5 Å structure of the whole ribosome from *T. thermophilus*, T70S<sup>6</sup> and the unbound D50S.<sup>7</sup> Note that this bridge stretches from the proximity of the decoding center (D) in the small subunit to the vicinity of the PTC (P)

**Plate 2.** Symmetry-related region, the rotatory motion and presumed D-amino acid positions. Blue and green represent the parts including the A-site and the P-site, respectively. The same color system applies to the tRNA acceptor stems and to 3' ends of ASM and of the rotated moiety (shown as atoms). (a) View of the symmetry related region down its rotation axis (marked by a red dot). RNA backbone is represented by ribbons. The core of the two-fold symmetry related region, including the PTC and the 3' ends of ASM and of the rotated moiety, is encircled in red. This core is shown in (b) and (f). A perpendicular view is shown in Plate 3(b). (b) A projection down the two-fold axis of the core of the symmetry related region [circled in (a)]. The red dot is the position of the rotation axis. Nucleotide A2602, the presumed 'propeller', is shown in magenta. (c–f) Snapshots of the spiral motion, obtained by successive rotations, by 15° each, of the rotating moiety from the A- to P-site, around the two-fold axis coupled with the appropriate fraction of the total spiral translation (2 Å). Note that both tRNAs ends point into the exit tunnel. The ribosomal components belonging to the PTC rear wall, which confine the exact path of the rotatory motion, are shown in gray or red. The PTC front wall conserved nucleotides, A2602 and U2585, are in magenta and pink, respectively. The A–P passage is represented by the transition from the A-site aminoacylated tRNA (in blue) to the P-site (in green). The blue-green round arrows show the rotation direction. (c) A view of the simulated rotatory motion perpendicular to the two-fold axis. (d) The same view as in (c), together with the suggested shift of the tRNA acceptor stem. The blue-green flat arrow shows the direction of the shift, whereas the blue-green round arrows show the direction of the rotatory motion. (e) and (f) Orthogonal to the views shown in (c) and (d). (e) A view from the tunnel into the PTC. (f) The rotatory motion down the two-fold axis, looking from the PTC towards the tunnel. Note the arched pattern scaffolded by the ribosome. (g) Graphical representation of peptide-bond formation. The 3' end of ASM is shown in blue and the derived P-site tRNA in green. The blue circle designates the nucleophilic amine and the red shows the center of the oxyanion. The small curved arrows represent a transfer of hydrogen, which should generate the oxyanion intermediate of the reaction. The blue arrow shows the transfer from the amine to the carbonyl carbon, and the green arrow follows the transfer from the intermediate to the leaving group. Bottom right four representations: the structural basis for the elimination of D-amino acid incorporation. Top: Two views of the PTC together with ASM and the simulated P-site substrate are shown on top. The reactants of the peptide bond formation, namely the A-site nucleophilic amine and the P-site carbonyl carbon are encircled. Bottom: The results of two attempts at modeling D-phenylalanine within the PTC, by overlapping a D-isomer on the ASM 3' end. Left: The black star indicates the short contact with U2506, obtained by overlapping the nucleophilic amine. Right: The red star indicates the possible hydrogen bond with U2585, obtained by superposition of the side-chains of the D-isomer and of the ASM amino acid

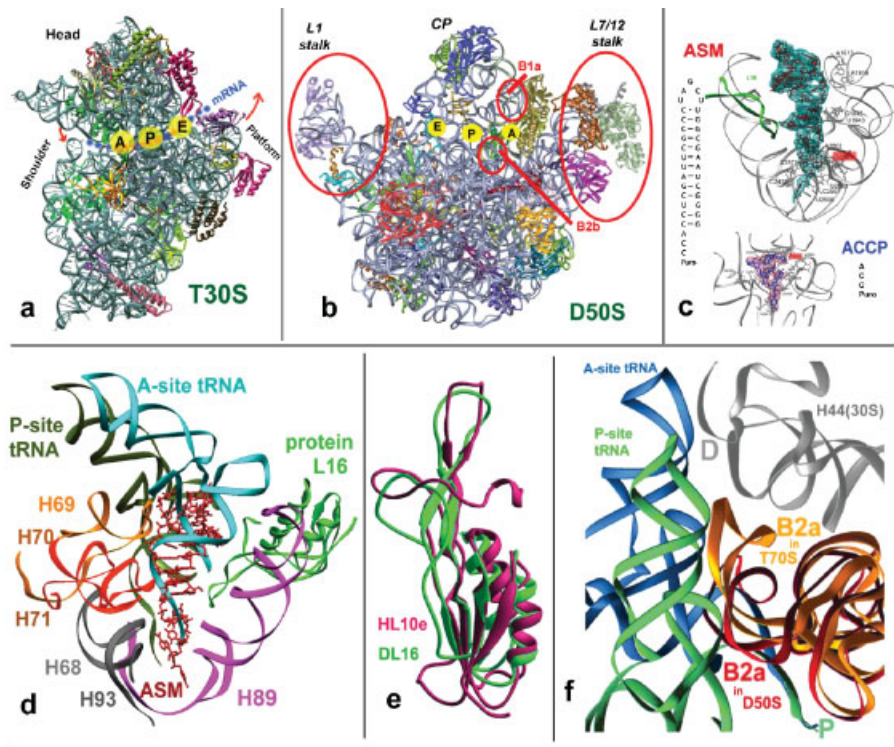


Plate 1

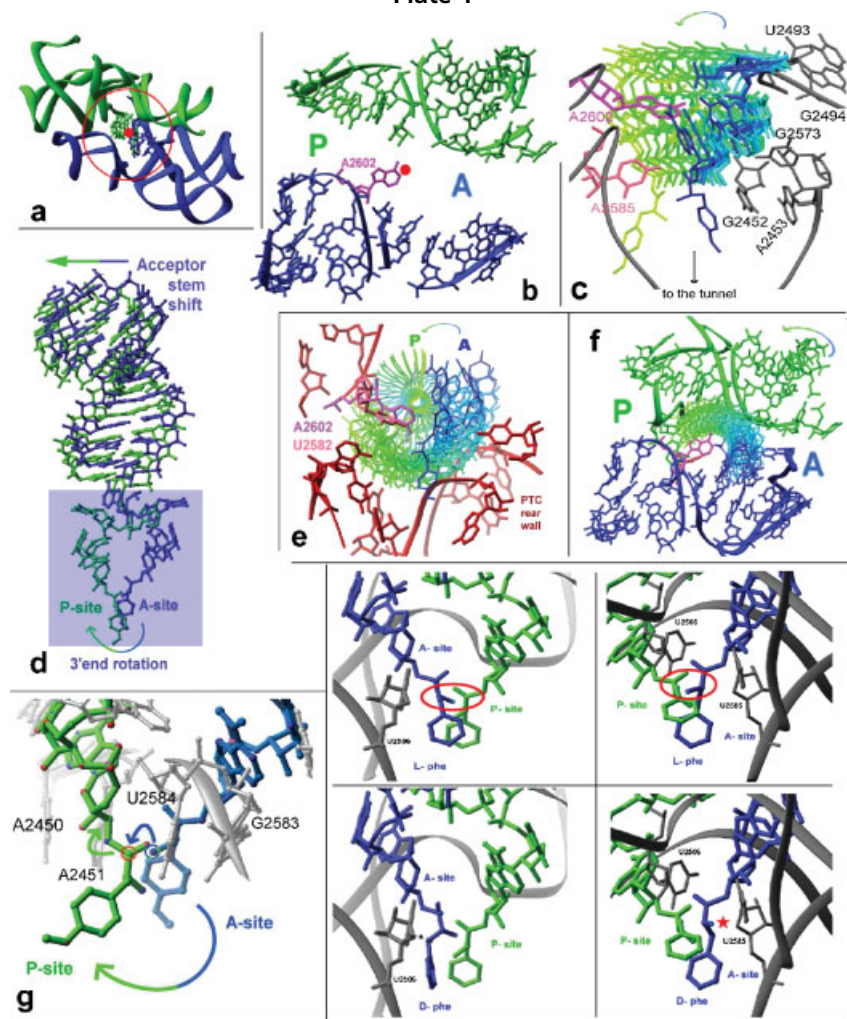
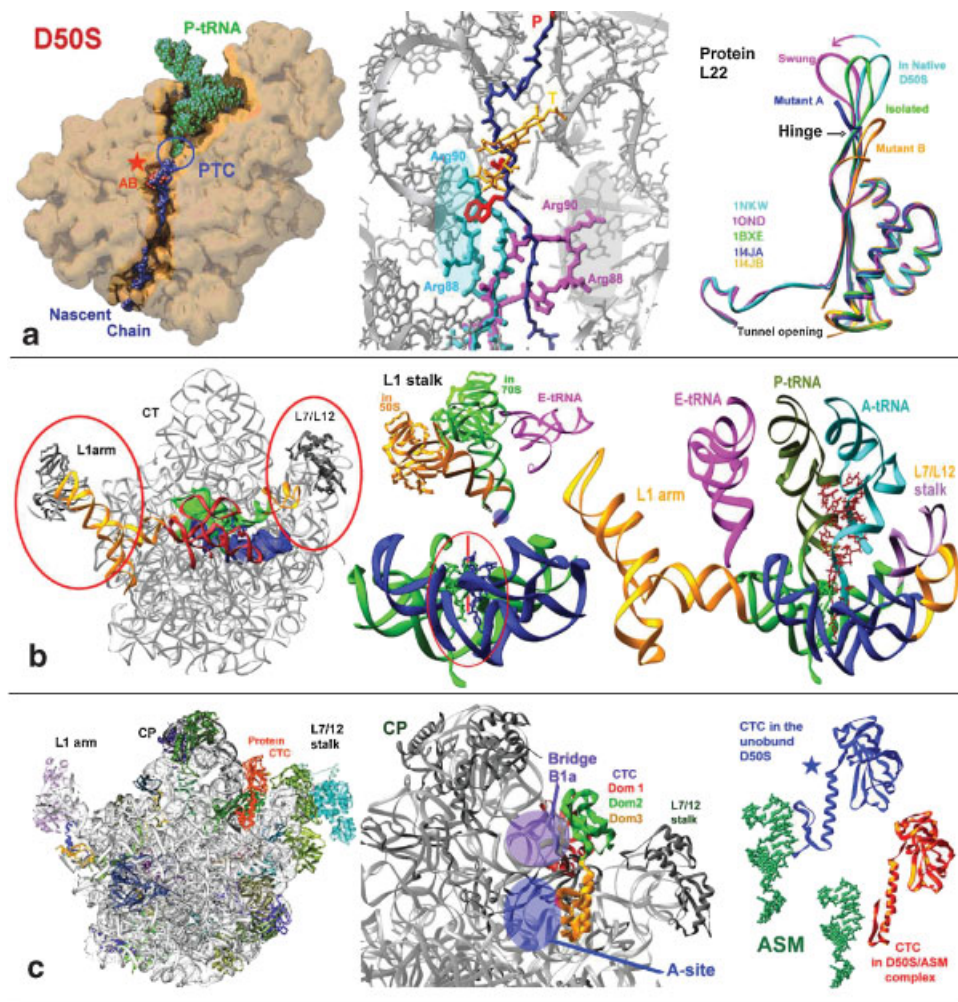


Plate 2



**Plate 3.** Ribosomal involvement in regulation and signal transmission. (a) Gating of the ribosomal tunnel by the tip of protein L22  $\beta$ -hairpin. Left: The overall view of the ribosomal tunnel and its position within the large ribosomal subunit (in orange-brown) together with docked P-site tRNA and a modeled growing peptide. The PTC and the site targeted by macrolide antibiotics are marked. Middle: A view parallel to the long axis of the ribosomal tunnel (ribosomal RNA shown in gray) together with the modeled progression of a polyaniline chain (blue), on which the positions of the two key residues for SecM arrest,<sup>35</sup> Pro and Trp are highlighted in red. The tip of the  $\beta$ -hairpin of protein L22 at its native conformation is shown in cyan, and the swung conformation in magenta. For comparison, TAO binding site is also shown (in gold). The gray and the cyan areas correspond to the regions containing the mutations in 23S RNA and in protein L22 (respectively) that bypass the elongation arrest of SecM protein.<sup>35</sup> Right: All known conformations of protein L22. Note the similarity of these structures, except for at the tip of the hairpin region. (b) The symmetry related region bridging remote ribosomal functional sites. Left: The location of the two-fold related region within the D50S structure (represented by its RNA backbone in gray). Shown are the symmetry related features [in blue (A-region) and green (P region)], as in plate 3, with their extensions (in gold and pink). The approximate large subunit portions confined by the symmetry related region are masked according to the same color code. The B2a intersubunit bridge [shown also in Plate 1(f)], which connects the PTC of the large subunit with the decoding center in the small subunit, is colored red. The location of this bridge at the border of the PTC cavity, hints at its potential role in transmitting signals between the two lateral protuberances of the large subunit, namely the tRNA entrance and exit sites, and the two ribosomal active sites: the PTC and the decoding center. Middle: The symmetry related region seen perpendicular to the view shown in Plate 2(a), with the same color code. The core of the two-fold symmetry related region, including the PTC and the 3' ends of ASM and of the rotated moiety [shown in Plate 2(b)], is encircled in red. Insert: The two crystallographically observed conformations of the L1 arm (including the RNA features H76-H78 and protein L1), which serves as the 'door' for E-site tRNA release: 'the closed state', as seen in the tRNA complexed T70S ribosome,<sup>6</sup> and the 'open state', as observed in the structure of the unbound large subunit, D50S.<sup>7</sup> The pivot between these structures is marked by a blue dot. The distance between the outer regions of this arm in the two structures is approximately 30 Å. E-site tRNA was added, in its location and orientation in the T70S ribosome complex.<sup>6</sup> Right: A detailed view of the left figure, showing the symmetry related region together with ASM (red), the rotated moiety (green, shown as atoms) and the docked A-, P- and E-site tRNAs (in cyan, green and pink, respectively). (c) CTC, a three domain regulatory protein. Left: The position of protein CTC within the ribosome. Middle: Zoom on the CTC vicinity. The three CTC domains are shown. Domain-1 (red) resembles protein L25;<sup>67</sup> domain-2 (green), which together with domain 1 forms a structure almost identical to that of protein TL5,<sup>68</sup> and domain-3 (gold), which is unique to *D. radiodurans*.<sup>7</sup> Highlighted are the approximate locations of the B1a intersubunit bridge (also known as the 'A-site finger' or helix H38) and of the acceptor stem of the A-site tRNA (in violet and blue, respectively). Right: The native and ASM (green) induced rearranged conformations of protein CTC C-terminal domain, are shown in blue and red-orange, respectively. The blue star indicates the flexible contact between the CTC middle and C-terminal domains

## Sizable symmetry related region within a giant asymmetric molecular machine

The ribosome is a giant asymmetric riboprotein particle. Yet, a large symmetry-related region, containing about 180 nucleotides, was revealed in all known structures of the large ribosomal subunit [Plate 2(a)].<sup>8,9,11</sup> This symmetry relates the backbone fold and nucleotides orientation [Plate 1(b)], rather than nucleotide type. The existence of a two-fold symmetry can be justified by the need to offer comparable supportive environments to two similar chemical moieties that have to face each other in order to allow participation of the A-site amine and the P-site carbonyl-carbon in peptide bond formation.

The axis of the symmetry related region is positioned close to the center of the PTC, between the A- and the P-loops, and points into the protein exit tunnel [Plate 2(b) and (c)]. In the structure of the complex of D50S with ASM,<sup>8</sup> the ribosomal symmetry axis nearly coincides with the bond connecting the ASM double helical features with its single-stranded 3' end, the moiety carrying the amino acid. It seems, therefore, that the A- to P-site passage involves two independent, albeit correlated, motions: a shift of the A-tRNA helical regions, performed as part of the overall mRNA/tRNA translocation, and a spiral rotation of the tRNA 3' end [Plate 2(d–f)], consistent with results of footprinting experiments, indicating spontaneous movement of the A-tRNA acceptor stem into the P-site.<sup>24</sup> This rotatory motion creates favorable stereochemistry for peptide-bond formation [Plate 2(g)] and seems to be performed in conjunction with the chemical reaction.<sup>8,9,11</sup>

Looking down the symmetry axis, the PTC appears as an arched void of a size sufficient to accommodate the tRNA-3' end. The shape of this void and its position seems to be designed as the path along which the rotatory motion of the A-site 3' end proceeds into the P-site [Plate 2(f)]. The PTC wall located away from the subunit interface, known as the rear wall, forms the scaffold that guides the rotatory motion. Two nucleotides, A2602 and U2585, which bulge into the center of the PTC from its front wall [Plate 2(d–f)], seem to play a pivotal role in directing the rotatory motion. A2602 is located at the upper side of the PTC and can interact with position 73 of the tRNA, the nucleotide connecting the 3' end and the rest of the tRNA. U2585 resides at the bottom of the PTC at the ribosomal exit tunnel.

The interactions of both the A- and the derived P-site tRNAs with the PTC, which represent the beginning and the end of the rotatory motion, are consistent with most of the available biochemical data.<sup>23–26</sup> While rotating, the A-site 3' end slides along the backbone of two rear-wall nucleotides and can interact with the rear-wall bases that point inward. In this way the PTC walls confine the precise path for the rotating moiety, and ensure that the rotating moiety arrives at the P-site at an optimal configuration for peptide bond formation. Importantly, the four

nucleotides of the P-site region, which are located by the tunnel entrance, are positioned somewhat lower ( $\approx 2$  Å) than their A-site mates, the rotatory motion thus acquiring a spiral nature, positioning the nucleophilic amine group facing the peptidyl carbonyl carbon and ensuring the entrance of the nascent proteins into their exit tunnel.

With its entrance adjacent to the PTC, this tunnel provides the path along which the growing polypeptide chains progress until they emerge out of the ribosome. Over 30 years ago, the existence of this tunnel was deduced from biochemical findings.<sup>27,28</sup> In the mid-1980s it was first observed by three-dimensional image reconstruction,<sup>29,30</sup> then re-visualized by cryo-electron microscopy<sup>31,32</sup> and recently reconfirmed by x-ray crystallography.<sup>3,6,7</sup> It spans the large ribosomal subunit and has a non-uniform diameter [Plate 3(a)]. At its entrance, the tunnel's diameter matches, almost precisely, the size of the bulky amino acid residues. It may therefore allow the passage of shorter or flexible amino acid residues to which small compounds are bound,<sup>33,34</sup> but seems to restrict motions of large side-chains or conformational rearrangements of rigid residues, such as proline. The tunnel entrance is the preferred target of a large number of clinically useful antibiotics, namely the macrolide, ketolides and azalide families [Plate 3(a)]. However, despite the utilization of a rather limited ribosomal region, and the tendency of the macrolide antibiotics to block the progression of the nascent proteins, significant variability was detected in their binding modes, the positions and the precise inhibitory mechanisms of different antibiotics, even among eubacteria.<sup>12,13,15,16</sup>

The rotatory motion, which could be simulated with no space constraints or steric hindrances, ends with a derived P-site tRNA located at a distance, orientation and stereochemistry suitable for peptide bond formation [Plate 2(g)].<sup>8,9,11</sup> A nucleophilic attack of the amino nitrogen of the aminoacylated-tRNA can readily occur at the pH found to be optimal for protein biosynthesis in almost all species, which is also the pH within the D50S crystals, since these are grown and maintained under close to physiological conditions.<sup>7,21</sup> A nucleophilic attack, performed while both the A- and the P-sites are still occupied by the aminoacylated-tRNA and the peptidyl-tRNA, respectively, will generate a tetrahedral oxyanion intermediate. The next steps of this reaction, namely  $sp^3$  to  $sp^2$  reorganization and a transfer of a hydrogen to the leaving group, which leads to the deacylation of the tRNA in the P-site, seems to occur in concert with the rotatory motion. The passage of the A-site tRNA 3' end into the P-site should assist the release of the leaving group, thus vacating the space for a new aminoacyl tRNA and securing the process of protein biosynthesis.

At the beginning of the biosynthetic process, the correct selection of the binding site and the mode of the first aminoacylated tRNA, which is a part of the initiation complex, to both subunits, is vital. The positioning of the first tRNA at the P-site of the small subunit is dictated by

the mRNA binding mode and the selection of the first codon on the mRNA.<sup>22</sup> The situation in the large subunit, however, is more complicated, since this subunit is not involved with any guideline. In principle, the first tRNA could be accommodated in the A- or the P-site, since both are free and available. However, analyzing the potential interactions in the two PTC binding sites, shows that compared with the A-site, the P-site contains an additional candidate for basepairing, namely G2252 with tRNA position 74. It seems that the importance of the double basepairing between the P-site and tRNA C74 and C75, alongside the known preference of tRNA synthetases for aminoacyladenylates, rationalize the universality of the CCA motif of the tRNA 3' end. Hence, it seems that besides accurate substrate positioning, the sole stereochemical requirement for extending the initiation process towards the creation of a peptide bond is that the initial P-site tRNA is at the orientation acquired at the end of the rotatory motion.

In short, a rotatory motion of the tRNA 3' end, concurrent with the shift of the major part of the A-tRNA molecule into the P-site, is the key component of a unified ribosomal mechanism for peptide-bond formation, translocation and nascent protein progression. According to this integrated ribosomal machinery, the peptide bonds are formed spontaneously, in an exothermic reaction, consistent with early suggestions, based on biochemical evidence.<sup>36</sup> The ribosome contributes positional catalysis to peptide bond formation as well as to polypeptide elongation: by providing the architectural means for accurate substrate positioning and alignment; by the design of an exact path for the A- to P-site passage; and by the guidance of the rotatory motion along this path. No ribosomal component is required for the mere chemical events of peptide bond formation, but specific ribosomal moieties could have a major influence on the rate of protein biosynthesis, which plays a key role in cell vitality,<sup>37,38</sup> as well as on the process following the formation of the peptide bond, namely the elongation of the nascent chains.

## Fragment Reaction

Puromycin is a universal ribosome inhibitor. In all ribosomes it competes with A-site tRNA binding, since its structure resembles that of the tip of aminoacylated tRNA [Fig. 1(b)], hence it has been exploited extensively in biochemical studies, aimed at shedding light on ribosomal function. Under specific conditions, the use of specific puromycin derivatives could lead to abnormal formation of a single peptide bond, by a yet unknown mechanism, called the 'fragment reaction'. Importantly, this reaction is about  $10^3$  times slower than the normal formation of peptide bonds,<sup>10</sup> and can be performed under conditions that are neither similar to those found to be optimal for *in vitro* protein biosynthesis, nor do they resemble the *in vivo* environment.

A dipeptide detected at the A-site within H50S crystals formed by the 'fragment reaction', led to a suggestion that A- to P-site passage follows peptide bond formation.<sup>39</sup> Such a sequence of events is bound to be impractical since it implies that the entire newly formed polypeptide, no matter what its length is, has to be rotated by  $180^\circ$  each time a peptide bond is being formed. Alternatively, the nascent chain exploits free rotations around its main-chain bonds in order to compensate for the  $180^\circ$  rotation of the tRNA 3' end carrying the nascent polypeptide. In view of the tunnel-entrance space limitations, rotations of bulky side chains, such as tryptophane, can create severe clashes, and the need for rearrangements of the nascent protein main-chain would rule out incorporation of rigid residues, such as proline. Furthermore, rotation or rearrangement should be exceedingly space consuming as well as extremely costly energetically, assets that are hardly provided during chain elongation and may not be compensated by the only energy source of protein biosynthesis, namely the EF-G (elongation factor G) induced GTP (guanine-3-phosphate) hydrolysis.

Thus, it seems that the creation of a dipeptide that remains at the A-site results from: improper positioning of its reactant, as observed for similar compounds in the absence of remote interactions;<sup>39-41</sup> the creation of a peptide bond under far from optimal reaction conditions (e.g.  $\text{pH} \approx 5.6$  instead of  $\approx 8$ <sup>10,39</sup> and relatively low salt concentrations<sup>2</sup> instead of the high salt required for *H. marismortui* efficient protein production<sup>21</sup>); the low affinity of puromycin derivatives to the P-site;<sup>10,39</sup> or because the reactants used for this 'fragment reaction' lack the bond around which the rotatory motion should occur.

## REGULATION, DISCRIMINATION AND SIGNALING

### Subunit association and PTC diversity

The correct assembly of functionally active ribosomes depends on accurate positioning of the two ribosomal subunits relative to each other. The contour of the interface regions of both ribosomal subunits show significant similarity, but this by itself is not sufficient for productive subunit association. Consequently, cells contain either active assembled ribosomes, or the two individual subunits. Once the initiation complex is ready for assembling with the large subunit to form the functional ribosome, an immediate creation of a stable functional organelle has to follow, and the intersubunit bridges together with the P-site tRNA, an integral part of the initiation complex, fulfill this requirement. These bridges are composed of components from both subunits and form upon their association by conformational rearrangements. There are structural indications that in most cases the large subunit portions of the bridges undergo larger rearrangements than those originating from the small subunit.<sup>9,41</sup>

It seems that the conformational mobility of these bridges is utilized by the ribosomes, not only for the creation of functional active ribosomes. It is conceivable that several intersubunit bridges facilitate the transitions of the ribosome into its various functional states. A striking example is the intersubunit bridge connecting the two ribosomal active sites, namely the decoding center in the small subunit and the PTC in the large one, called B2a or H69. Its proximity to both the A- and the P-site tRNAs and its two different conformations, both observed crystallographically<sup>6,7</sup> [Plate 1(f)], suggest that it could also participate in translocation, presumably by acting as a crane or a platform to assist the shift of the A-site tRNA helical regions.<sup>8,9,11</sup>

The large subunit component of the B2a bridge, the tip of Helix H69, is also a part of the walls of the cavity hosting the PTC [Plate 1(c) and (d)]. As such, it is a major participant in the remote interactions that govern the accurate positioning of the tRNA substrates.<sup>8,9,41</sup> The crucial contribution of H69 interactions to productive alignment of the A-site tRNA substrate is demonstrated by the finding that in their absence similar, albeit distinctly different, binding modes were observed within the PTC,<sup>39–41</sup> all requiring conformational rearrangements in order to participate in peptide bond formation.<sup>10</sup> Lack of remote interactions could be due to the disorder of H69, as observed in the H50S high-resolution structure,<sup>2,3</sup> or result from the use of tRNA analogues that are too short to reach the upper rim of the PTC cavity, where the components providing the remote interactions reside.<sup>39,40</sup>

The structures of the substrates bound ribosome<sup>6</sup> and to the large subunit, D50S,<sup>8</sup> indicate that similar to Helix H69, protein L16 is also involved in moderating accurate substrate positioning. This protein is located at the upper rim periphery of the PTC cavity [Plate 1(c)], in a position allowing interactions with the acceptor stem of the A-site tRNA, and these remote interactions appear to be of major importance. As expected for ribosomal components involved in dominating key functional tasks such as substrate placement, its three-dimensional structure is conserved between eubacteria (represented by D50S)<sup>7</sup> and archaea (represented by H50S<sup>2</sup>), although the amino acid sequences of L16 and of its partner from the archaeon *H. marismortui*, L10e [Plate 1(a)], show poor homology. The governing of substrate placement by remote interactions seems to be designed to control the correct substrate alignment while allowing diversity at the PTC active site. Flexibility and variability seem to be crucial for the PTC function, consistent with the need to host aminoacylated tRNA 3'ends of various sizes and different chemical natures.

The ability of the ribosome to accommodate semi-reactive substrate-analogues, inhibitors and compounds supposed to represent reaction-intermediates,<sup>3</sup> does not imply that each of the bound compounds could participate in amino acid polymerization, although under specific circumstances, a single peptide bond can be formed

by the 'fragment reaction'.<sup>39</sup> It appears that, in general, the orientations of reactants that are not placed by remote interactions could be incompatible with polypeptide elongation. Furthermore, almost all of the substrate-analogues mimicking only the tRNA 3' end were found to necessitate conformational rearrangement in order to participate in peptide bond formation and/or chain elongation. Such rearrangements should require time, justifying the lower rate of the 'fragment reactions'<sup>10</sup> compared with normal protein biosynthesis, and could be assisted by the PTC mobility, in which the conserved A2602 seems to play a key role. It was shown that this base adopts a different orientation in each of the known complexes of the large subunit and its striking conformational variability appears to be synchronized with the rotatory motion.<sup>8,9,11</sup> Consequently, nucleotide A2602 was proposed to act as a conformational switch within the PTC, propelling the rotating moiety in concert with the action of helix H69, the feature that appears to assist the shift of the tRNA acceptor stem, at the subunit interface.<sup>11,41</sup>

Despite the PTC high conservation, variability of its conformation resulting from alterations of parameters such pH, temperature and ion concentration, has been suggested, based on biochemical findings, over three decades ago.<sup>42–44</sup> These observations were confirmed recently by several methods, including chemical probing<sup>45</sup> and cryo-electron microscopy studies, investigating the effect of buffer composition on tRNA-ribosome interactions.<sup>46</sup> Consistently, conformational differences were observed by comparing the available crystal structures that were determined under various conditions.<sup>2,6,7</sup> Actual modifications in the ribosomal RNA sequence within the PTC have less influence on the PTC overall conformation, since its backbone obeys the local two-fold symmetry.<sup>8,9,11</sup>

Correlation between the ribosomal functional state and the conformation of its PTC has been suggested, based on functional, biochemical and genetic evidence.<sup>42,45</sup> Consistently, disorder in the H50S crystal structure,<sup>2</sup> observed despite the high level of order within the ribosomal core, could be correlated with the environment of the crystal, which is far from that leading to efficient protein biosynthesis.<sup>21</sup> It is conceivable that disorder of functionally relevant components is induced by the ribosome itself, aimed at avoiding unproductive subunit association and substrate binding, when the conditions are not suitable for efficient operation. Hence, the disorder seen in the H50S structure could indicate a common ribosomal strategy for securing cell efficiency.<sup>21</sup>

### Transmitting intra-ribosome functional signals

Connecting the two ribosomal active sites, bridge B2a seems to be designed for transmitting signals between them. The symmetry related region is an additional

feature that is likely to participate in intra-ribosomal functional signaling. This region is positioned between the two lateral protuberances of the large ribosomal subunit [Plates 1(b) and 4(b)], and includes in its inner core the PTC and its immediate neighborhood, which occupy about a fifth of its nucleotides [Plate 2(a) and (b)]. The extensions of this region beyond the PTC reach the highly flexible L7/L12, the location used for A-site tRNA entrance, and the pivot of the L1 stalk, the feature designated as the 'door' for the E-site tRNA release. Both stalks possess significant conformational flexibility and are presumed to undergo cooperative motions, thus enabling the entrance and the exit of aminoacylated and deacylated free tRNA, respectively [Plate 3(b)].<sup>7,21</sup>

It seems, therefore, that the outer shells of the symmetry related region play roles in amplifying the stabilization of the symmetry related region, and in facilitating signaling between the incoming and leaving tRNA molecules,<sup>9,11</sup> thus being responsible for an essential path of intra-ribosomal functional information transfer. In this capacity these extension can provide means for ribosomal control of substrates trafficking between the three tRNA sites on the large subunit, a motion that must be coordinated with the advance of the mRNA on the small subunit. Interacting with the PTC cavity, which contains bridge B2a at its upper rim, the symmetry related region could also provide the machinery for information flow between the active centers of the two subunits [Plate 3(b)].

### Controlling the elimination of D-amino acids

All proteins synthesized by ribosomes are built solely of L-isomers of the amino acids, despite the occurrence of D-amino acids (D-aa) in cells. It was shown that crude extracts of several organisms, such as bacteria, yeast and mammals contain enzymatic activity capable of hydrolyzing the ester bond of D-Tyr-tRNA, and that *E. coli* and *Bacillus subtilis* tyrosyl-tRNA synthetases are able to charge tRNA by D-tyrosine *in vitro*.<sup>47</sup> Free D-tyrosine is likely to be generated by the catabolic turnover of the dipeptide DL-dityrosine residing in the *S. cerevisiae* wall.<sup>48</sup> In general, free D-aa are toxic to numerous organisms. These protect themselves against the toxicity by enzymes such as D-serine deaminase that metabolizes D-serine.<sup>49</sup> The cells utilize their D-amino acids for specific cellular activities<sup>50</sup> other than protein biosynthesis, and in order to avoid the incorporation of D-aa into proteins, the cells have developed various mechanisms. Most of these mechanisms eliminate the usage of the D-aa during stages prior to the ribosomal translation of the genetic code, such as aminoacylation of tRNAs by the synthetases and binding of aminoacyl-tRNAs to elongation factors.<sup>51</sup>

The occurrence of D-aa in living cells could lead to mistakes during protein biosynthesis. However, naturally produced proteins containing D-isomers do not exist in living cells. Consistently, analogues containing D-aa were

shown to function poorly as donors in protein biosynthesis<sup>52</sup> and despite repeated efforts the D-isomers could not be incorporated into proteins *in vivo*.<sup>53</sup> Owing to the PTC significant tolerance for substrate binding,<sup>8,11,41</sup> one would expect that a D-amino acid could be accommodated by the PTC. Hence the exclusivity of the L-isomer in proteins points to the existence of a ribosomal mechanism to avoid this mistake. This exclusion mechanism should function satisfactorily despite the natural conformational flexibility of the PTC, and suggests that for the incorporation of D-aa in a growing polypeptide the PTC should be modified extensively and loose its D-aa rejecting mechanism, consistent with a recent report indicating enhanced D-aa incorporation into protein by ribosomes mutated at the PTC or in its vicinity.<sup>54</sup>

In order to analyze the factors that may be involved in D-aa rejecting mechanisms, we examined the high-resolution structure of the PTC in its native form, within D50S,<sup>7</sup> and in a complex with several substrate analogues.<sup>8</sup> We used ASM [(Fig. 1(b) and Plate 2(c) and (g)] position in D50S as a reference, as it binds to the PTC in a productive manner, in a configuration allowing peptide bond formation,<sup>8,9,11</sup> and replaced its original L-tyrosine by modeled L- or D-phenylalanine. We found that overlapping the nucleophilic amine and preserving its proper stereochemistry, would lead to a collision between the C<sub>β</sub> of the D-enantiomer and O4' of U2506. The alternative model, obtained by superposition of the side-chains of the D-isomer and of the ASM amino acid, led to an overlap of the carbonyl groups, combined with a flip of the nucleophilic amine towards the PTC wall. Consequently, instead of being within the distance and in the orientation suitable for nucleophilic attack, the amine of the D-isomer is located within a hydrogen bond distance from U2585 [Plate 2(h)]. Such a hydrogen bond could hamper a possible rotation of the amine group towards its proper attacking position. U2585, the nucleotide that seems to have the ability to 'lock' the D-aa in an unproductive orientation, is a universally conserved nucleotide, shown to be exceedingly important for the maintenance or the destruction of the PTC active conformation and for anchoring the rotatory motion. In the native D50S structures, and in its complexes with correctly placed L-isomer aminoacylated tRNAs, U2585 is part of the PTC front wall [Plate 2(c), (e) and (f)]. Although a lower number of conformations were observed for it, compared with A2602, the suggested propeller of the rotatory motion,<sup>9,11,21,41</sup> U2585 could undergo substantial conformational change in its base orientation. Thus, a 180° rotation of its base was observed upon binding of dalfopristin, the component of the synergetic antibiotic Synercid<sup>®</sup> that binds to the PTC. This non-productive U2585 conformation, can, in turn, be stabilized by the binding of quinupristin, the second Synercid<sup>®</sup> component, thus leading to a prominent synergetic effect.<sup>14</sup>

We conclude, therefore, that the PTC interference with D-aa incorporation into a growing chain is based

on space considerations as well as on the creation of unproductive interactions, which could be irreversible. Substantial conformational rearrangements within the PTC could bypass both mechanisms, consistent with the suggestion based on mutation experiments.<sup>54</sup> In these experiments, two regions were mutated: the PTC (nucleotides 2447–2450) and in Helix H89 (2457–2462). Among these, according to our analysis, the appropriate candidates for inducing conformational alterations enabling D-isomer bindings are nucleotides U2449 and A2450.

### Tunnel discrimination of nascent proteins

Recent crystallographic studies indicated that the ribosomal exit tunnel, assumed to be a passive path for nascent proteins,<sup>3</sup> possesses intrinsic conformational mobility meaning it could be blocked.<sup>15</sup> This tunnel was shown to undergo alterations associated with antibiotics resistant mutations,<sup>55</sup> to possess discriminating properties<sup>35,56,57</sup> and to actively participate in regulating intracellular cotranslational processes.<sup>58–60</sup> Experiments with the secM (secretion monitor) protein,<sup>35</sup> and the leader peptide of *E. coli* tryptophanase (tnaC) operon<sup>57</sup> are of particular interest. The sequences of both proteins contain a similar motif, which causes elongation arrest under specific conditions, in conjunction with the existence of cellular systems to which they belong. For instance, SecM is produced only in the presence of a protein-export system, shown to recognize an export signal located at the nascent chain. When this protein-export system is damaged or absent, elongation arrest occurs. In both proteins this signal is a sequence-motif located in the N-terminus (about 150 residues away in secM protein), and is characterized by its composition. The main features of this motif are a tryptophane and a proline, separated by  $\approx 12$  residues.

Mutations in the ribosomal protein L22 hairpin tip and in the 23S rRNA were shown to alleviate the elongation arrest in SecM protein.<sup>35</sup> These arrest-bypassing mutations were mapped on the large ribosomal subunit, D50S, as well as on the structure of its complex with the antibiotic troleandomycin (TAO),<sup>15</sup> a semi-synthetic macrolide that contains no hydroxyl moieties,<sup>61</sup> and is hence unable to form the typical macrolides (e.g. erythromycin) hydrogen bonds.<sup>12</sup> Similar to other macrolides,<sup>12–16,62</sup> TAO binds to the exit tunnel, close to its entrance.<sup>15</sup> It exploits the macrolide favorable binding site, namely the vicinity of A2058, in a rather unique fashion [Plate 3(a)], presumably dictated by its size and chemical properties. Compared with erythromycin, it is located somewhat deeper in the tunnel and instead of being nearly perpendicular to the tunnel wall, it is almost parallel to it. Reaching into the domains far from the main macrolides binding region, TAO is similar to the azalides and ketolides.<sup>13,16</sup>

At its unique binding orientation, TAO hits an element of the tunnel wall, the tip of protein L22  $\beta$ -hairpin, a tunnel constituent reaching from close to the PTC to the vicinity of the tunnel opening on the other side of the large subunit.<sup>3,7</sup> This tip consists of 11 residues and contains at its very end an amino acid triplet (*E. coli* residues 88–90) that can act as a ‘double hook’ interacting with the RNA, since it is composed of a highly conserved arginine, an invariant alanine, and a residue that is in most species either an arginine or a lysine. In the native large-subunit structure, most of the ‘double hook’ is embedded in a narrow groove, so that the space available for its conformational rearrangements is rather limited. Consequently, TAO binding causes a swing of the entire L22 hairpin tip across the tunnel [Plate 3(a)]. As the native conformation, the resulting swung conformation is well accommodated on the tunnel walls, being stabilized mainly by electrostatic interactions and hydrogen bonds.<sup>15</sup> Importantly, the region of the tunnel wall that interacts with the L22 hairpin tip at its swung conformation, seems to be designed for these extensive interactions, indicating that the L22  $\beta$ -hairpin tip swinging could be a general tunnel mechanism.

A striking correlation was observed between the locations of the SecM arrest-suppressing mutations and the ribosomal regions involved in the interactions of the tunnel walls with the L22 hairpin tip, at its swung conformation. Furthermore, all L22 mutations that bypass SecM elongation arrest were found to reside in the L22 hairpin tip. It is conceivable, therefore, that the L22 hairpin tip swinging mechanism, revealed by TAO binding, represents the means by which the ribosome exploits SecM for tunnel arrest, or other natural arrest mechanisms.<sup>9,11,15</sup>

Protein L22 has an elongated shape and lines the tunnel wall, extending from the tunnel entrance to the vicinity of its opening [Plate 3(a)]. Remarkably, this rather unusual elongated shape is also maintained in the isolated native<sup>63</sup> and mutated protein.<sup>64</sup> Furthermore, in all known L22 structures flexibility was observed only in the hairpin tip hinge region [Plate 3(a)]. The electrostatic properties of the surface of protein L22 support the suggestion for a common mechanism for tunnel blockage accomplished by swinging of L22 hairpin tip. The efficiency of this swinging depends on its accuracy, which is dictated by the positioning of L22 hinge region. A pronounced patch of positively charged amino acids, detected adjacent to the L22 hinge region,<sup>63</sup> seems to dominate the precise positioning of the hinge region of the L22 hairpin stem, which, in turn, should facilitate an accurate swinging motion and a successful anchoring of the ‘double-hook’ to both sides of the tunnel.

Within D50S, a single  $\beta$ -strand chain connects the tip of protein L22 hairpin, and the region of this protein, residing in the vicinity of the tunnel opening, on the surface of the ribosome, over 70 Å away. In this location

the C-terminus of L22 could interact with the 'pulling protein' and transmit signals according to which the swinging could be induced or eliminated, in a yet unknown mechanism. The SecM nascent chain can also participate in signal transmission, since by the incorporation of  $\approx 150$  residues it should reach the tunnel opening. The studies showing that signal transmitted through growing chains could be correlated with structural alterations in a membranal translocon pore that lines up directly with the exit tunnel,<sup>58</sup> support this suggestion.

We therefore concluded that a swing of L22  $\beta$ -hairpin tip, similar to that induced by TAO action, is a universal mechanism for tunnel gating, and that protein L22 is a major player in tunnel discrimination. Furthermore, protein L22 and the already formed portion of the nascent chain could be involved in transmitting signals from the environment into the ribosomal core. Thus, the cellular signals do not only induce tunnel blockage and elongation arrest, they can also control and monitor the reverse hinge motions, required for alleviation of the arrest by allowing sufficient space for nascent protein progression.

### Regulation under stressful conditions: protein CTC

*D. radiodurans* is an extremely robust gram-positive eubacterium, originally identified as a contaminant of irradiated canned meat. Although this bacterium shares striking sequence similarity with *E. coli*, it survives under a large range of mild and extreme growth conditions, and was isolated from environments of either excessive or very poor in organic nutrients, such as weathered granite in a dry Antarctic valley, room dust, wastes from atomic piles and irradiated medical instruments. It contains almost all systems for DNA repair, DNA damage export, desiccation, starvation recovery and genetic redundancy, and its genomic DNA is packed in an ultra-dense organization, enabling the accommodation of ionizing, ultraviolet and x-radiation.<sup>65,66</sup>

Despite its striking survival properties, significant similarity was detected between *E. coli* and *D. radiodurans* ribosomes. Being similar to *E. coli*, the best characterized biochemically and functionally ribosome source, the D50S crystal structure provides an excellent system for ribosomal structure–function correlations. Furthermore, as an ultimate survivor under stressful conditions, the modes of binding of substrate analogues to D50S should shed light on some cellular regulating mechanisms employed under starvation.

A ribosomal protein, known as CTC in *D. radiodurans*, was proposed by us to be involved in starvation regulation, since it undergoes substantial conformational changes upon ASM binding to D50S. CTC is one of the D50S novel features, replacing the *E. coli* protein L25 and its *T. thermophilus* homologue, TL5. Among the known members of the CTC protein family, the CTC from *D.*

*radiodurans* is the longest. It is built of three domains, two of which can play a role in survival mechanisms.<sup>7,9</sup> In D50S, protein CTC stretches from the solvent side over the gap between the 5S and the L11 arm towards the PTC on the large subunit front side [Plate 3(c)].

In D50S, the CTC *N*-terminal domain (*N*-CTC) is located on the solvent side, behind the intersubunit bridge B1a, also known as the A-site finger or H38<sup>6</sup> and interacting with the 5S RNA. As its structure is similar to that of the isolated protein L25 from *E. coli* in complex with 5S RNA,<sup>67</sup> it is likely that its location coincides with that of L25 in the *E. coli* ribosome. The *N*-CTC and the CTC middle domain (*M*-CTC) wrap a large part of the B1a bridge [Plate 3(c)], which, similar to all other bridges, is highly flexible and can readily become disordered, as seen in the structure of H50S.<sup>2</sup> The fold of a hypothetical D50S protein, built from the CTC *N*-terminal and middle domains is almost identical to the fold of the two-domain protein TL5 from *T. thermophilus*.<sup>68</sup> The slight changes in the relative orientations of the two domains in the two proteins can be correlated with crystal vs ribosome environments. Hence, it seems that TL5 occupies the same position, namely wraps around a B1a bridge, in the *T. thermophilus* ribosome.

Based on the position of *N*-CTC on the backside of the central protuberance, we suggest that this domain, and its partner L25, provides general protection to the B1a bridge. Further protection can be provided by *M*-CTC, or the *C*-terminal domain of TL5, as this domain wraps around this bridge, and is thus capable of preventing its sliding or spinning. It is conceivable that in the absence of this extra protection, such uncontrolled, or non-functional, movements are likely to occur at the elevated temperatures that are required for efficient functioning of *T. thermophilus* ribosome.

The *C*-terminal domain of CTC (*C*-CTC) is placed at the rim of the intersubunit interface, reaching the location assigned to the acceptor stem of the docked A-site tRNA,<sup>7,9</sup> in a position that should restrict the space available for the A-site tRNA. This CTC domain is connected to *M*-CTC by a slender linker that seems to be highly flexible [Plate 3(c)], thus permitting global conformational rearrangements. Indeed, repositioning of the entire *C*-terminal domain was observed upon ASM binding [Plate 3(c)]. This motion was presumably induced by A-site occupation in order to avoid collisions that could have occurred if *C*-CTC would have maintained its native position. Thus, the *C*-terminal domain of CTC seems to serve as an A-site tRNA binding regulator<sup>7,9,21</sup> exploiting a mechanism based on space exclusion. This is combined with the dynamics required for quick alterations from the *C*-CTC native conformation, which should exclude A-site binding, to the *C*-CTC conformation that frees the space required for substrate binding.

The positioning, mobility and the unique combination of structural similarities with the corresponding proteins

from various sources, could indicate that each of the three domains of CTC has a specific function. The interactions of CTC with the solvent side of the large subunit central protuberance, its ability to manipulate the A-site tRNA binding and its assumed contribution in enhancing the stability of the B1b intersubunit bridge, could be connected with the mechanisms that *D. radiodurans* developed for survival, and could hint at a possible connection between the CTC N-, M- and C-domains and life under mild, thermophilic and stressful conditions, respectively.

## CONCLUSIONS

Comparative analysis of the crystal structures of free and complexed ribosomal particles revealed an elaborate architectural-design that contains a sizable symmetry-related region within the otherwise asymmetric ribosome. This region stretches between the sites involved in the entrance and exit of the aminoacylated and free tRNAs (respectively), contains the PTC and interacts through the PTC periphery with the intersubunit bridge that reaches the decoding site in the small subunit. Located at the bottom of an elongated cavity, the PTC can accommodate various substrate analogues, as it contains the mobility for their rearrangements. However, despite the PTC tolerance, accommodation of D-amino acids is basically impossible, due to its potential interactions with U2585, a universal nucleotide residing on the PTC wall, which would lock it in non-productive conformation.

Structural elements of this design guide the passage of the tRNA 3' end within the PTC from the A- to the P-site, by a spiral rotatory motion. This motion is part of the translocation event, a fundamental act of the elongation cycle that could be performed by a straightforward shift,<sup>69–71</sup> or by incorporating intermediate hybrid states.<sup>72</sup> Within the PTC cavity, the rotatory motion of the tRNA 3' ends is likely to be propelled by A2602, an action connected to the shifts of the tRNA helical stems, which seem to be performed by the intersubunit bridge B2a, functioning as a molecular platform. A2602 and U2585, two universal nucleotides positioned in the middle of the PTC pattern, near the two-fold rotation axis, anchor the rotatory motion of the tRNA 3' end. This rotating moiety progresses along a ribosomal pattern and results in optimal stereochemistry for peptide bond formation, a reaction that can occur spontaneously at the pH of almost all living cells, and is likely to take place in concert with the rotatory motion. As the rotatory motion leads to a geometry facilitating the entrance of growing polypeptides into the exit tunnel, the polymerization of the amino acids into proteins proceeds smoothly and efficiently.

The following have all led to the suggestion of a universal unified ribosomal machinery that integrates peptide bond formation, translocation and nascent protein progression: the domination of remote interactions in the

precise positioning of the ribosomal substrates, which seems to be designed to overcome the PTC conformational variability; the PTC structural elements that provide the means to avoid the incorporation of the D-isomer of the amino acids; the overlap of the axis of the symmetrical region with the bond connecting the tRNA 3' end with its double helical regions; the scaffold guiding the rotatory motion associated with the A to P-site passage; and the match between the contour of the tRNA rotating moiety and the shape of the PTC rear wall.

Ribosomes can respond to cellular conditions during all stages of protein biosynthesis. Starvation can lead to a lower level of tRNA incorporation, and damage in the secretion monitoring systems can cause elongation arrest. We have shown that in addition to structure stabilization and substrate positioning, ribosomal proteins participate in several regulatory and quality control tasks. Examples are protein L22 that can be triggered to undergo a swinging motion resulting in the blockage of the exit tunnel, which limits or stalls nascent protein progression, and protein CTC, a multi-domain protein that is likely to stabilize intersubunit bridge movements at elevated temperatures (e.g. thermophilic bacteria) and contribute to cell survival under stressful conditions by regulating aminoacylated tRNA binding.

## Acknowledgements

Thanks are due to: J. M. Lehn, P. Ahlberg, M. Lahav, H. Gilon and W. Bennett for critical discussions; F. Franceschi and P. Fucini for supplying crystals; and M. Peretz, R. Albrecht and M. Laschever, for their contributions to different stages of this work. X-ray diffraction data were collected at ID19/SBC/APS/ANL and ID14/ESRF-EMBL. The US National Institute of Health (GM34360), the German Ministry for Science & Technology (BMBF05-641EA) and the Kimmelman Center for Macromolecular Assemblies, provided support. A.Y. holds the Helen and Martin Kimmel Professorial Chair.

## REFERENCES

1. Yonath A, Muessig J, Tesche B, Lorenz S, Erdmann VA, Wittmann HG. *Biochem. Int.* 1980; **1**: 428–435.
2. Ban N, Nissen P, Hansen J, Moore PB, Steitz TA. *Science* 2000; **289**: 905–920.
3. Nissen P, Hansen J, Ban N, Moore PB, Steitz TA. *Science* 2000; **289**: 920–930.
4. Schluenzen F, Tocilj A, Zarivach R, Harms J, Gluehmann M, Janell D, Bashan A, Bartels H, Agmon I, Franceschi F, Yonath A. *Cell* 2000; **102**: 615–623.
5. Wimberly BT, Brodersen DE, Clemons WM Jr, Morgan-Warren RJ, Carter AP, Vornrhein C, Hartsch T, Ramakrishnan V. *Nature* 2000; **407**: 327–339.
6. Yusupov MM, Yusupova GZ, Baucom A, Lieberman K, Earnest TN, Cate JH, Noller HF. *Science* 2001; **292**: 883–896.
7. Harms J, Schluenzen F, Zarivach R, Bashan A, Gat S, Agmon I, Bartels H, Franceschi F, Yonath A. *Cell* 2001; **107**: 679–688.

8. Bashan A, Agmon I, Zarivach R, Schluenzen F, Harms J, Berisio R, Bartels H, Franceschi F, Auerbach T, Hansen HA, Kossoy E, Kessler M, Yonath A. *Mol. Cell* 2003a; **11**: 91–102.
9. Bashan A, Zarivach R, Schluenzen F, Agmon I, Harms J, Auerbach T, Baram D, Berisio R, Bartels H, Hansen HA, Fucini P, Wilson D, Peretz M, Kessler M, Yonath A. *Biopolymers* 2003b; **70**: 19–41.
10. Moore PB, Steitz TA. *RNA* 2003; **9**: 155–159.
11. Agmon I, Auerbach T, Baram D, Bartels H, Bashan A, Berisio R, Fucini P, Hansen HA, Harms J, Kessler M, Peretz M, Schluenzen F, Yonath A, Zarivach R. *Eur. J. Biochem.* 2003; **270**: 2543–2556.
12. Schluenzen F, Zarivach R, Harms J, Bashan A, Tocilj A, Albrecht R, Yonath A, Franceschi F. *Nature* 2001; **413**: 814–821.
13. Schluenzen F, Harms JM, Franceschi F, Hansen HA, Bartels H, Zarivach R, Yonath A. *Structure* 2003; **11**: 329–338.
14. Harms JM, Schluenzen F, Fucini P, Bartels H, Yonath A. *BMC Biol.* 2004; **2**(4): 1–10.
15. Berisio R, Schluenzen F, Harms J, Bashan A, Auerbach T, Baram D, Yonath A. *Nat. Struct. Biol.* 2003a; **10**: 366–370.
16. Berisio R, Harms J, Schluenzen F, Zarivach R, Hansen HA, Fucini P, Yonath A. *J. Bacteriol.* 2003b; **185**: 4276–4279.
17. Stark H, Orlova EV, Rinke-Appel J, Junke N, Mueller F, Rodnina M, Wintermeyer W, Brimacombe R, van Heel M. *Cell* 1997; **88**: 19–28.
18. Gabashvili IS, Agrawal RK, Grassucci R, Squires CL, Dahlberg AE, Frank J. *Embo. J.* 1999; **18**: 6501–6507.
19. Pioletti M, Schluenzen F, Harms J, Zarivach R, Gluehmann M, Avila H, Bashan A, Bartels H, Auerbach T, Jacobi C, Hartsch T, Yonath A, Franceschi F. *Embo. J.* 2001; **20**: 1829–1839.
20. Zarivach R, Bashan A, Schluenzen F, Harms J, Pioletti M, Franceschi F, Yonath A. *Curr Protein Peptid Sci.* 2002; **3**: 55–65.
21. Yonath A. *Annu. Rev. Biophys. Biomol. Struct.* 2002; **31**: 257–273.
22. Ramakrishnan V. *Cell* 2002; **108**: 557–572.
23. Kim DF, Green R. *Mol. Cell* 1999; **4**: 859–864.
24. Wilson KS, Noller HF. *Cell* 1998; **92**: 337–349.
25. Moazed D, Noller HF. *Nature* 1989; **342**: 142–148.
26. Green R, Noller HF. *Annu. Rev. Biochem.* 1997; **66**: 679–716.
27. Malkin LI, Rich A. *J. Mol. Biol.* 1967; **26**: 329–346.
28. Sabatini DD, Blobel G. *J. Cell. Biol.* 1970; **45**: 146–157.
29. Milligan RA, Unwin PN. *Nature* 1986; **319**: 693–695.
30. Yonath A, Leonard KR, Wittmann HG. *Science* 1987; **236**: 813–816.
31. Frank J, Zhu J, Penczek P, Li Y, Srivastava S, Verschoor A, Radermacher M, Grassucci R, Lata RK, Agrawal RK. *Nature* 1995; **376**: 441–444.
32. Stark H, Mueller F, Orlova EV, Schatz M, Dube P, Erdemir T, Zemlin F, Brimacombe R, van Heel M. *Structure* 1995; **3**: 815–821.
33. Eisenstein M, Hardesty B, Odom OW, Kudlicki W, Kramer G, Arad T, Franceschi F, Yonath A. In *Supramolecular Structure and Function*, Pifat G (ed). Balaban Press: Rehovot, 1994; 213–246.
34. Kurzchalia TV, Wiedmann M, Breter H, Zimmermann W, Bauschke E, Rapoport TA. *Eur. J. Biochem.* 1988; **172**: 663–668.
35. Nakatogawa H, Ito K. *Cell* 2002; **108**: 629–636.
36. Nierhaus KH, Schulze H, Cooperman BS. *Biochem. Int.* 1980; **1**: 185–192.
37. Katunin V, Muth G, Strobel S, Wintermeyer W, Rodnina M. *Mol. Cell.* 2002; **10**: 339–346.
38. Rodnina MV, Wintermeyer W. *Trends. Biochem. Sci.* 2001; **26**: 124–130.
39. Schmeing TM, Seila AC, Hansen JL, Freeborn B, Soukup JK, Scaringe SA, Strobel SA, Moore PB, Steitz TA. *Nat. Struct. Biol.* 2002; **9**: 225–230.
40. Hansen JL, Schmeing TM, Moore PB, Steitz TA. *Proc. Natl. Acad. Sci. USA* 2002b; **99**: 11670–11675.
41. Yonath A. *Chem. Bio. Chem.* 2003; **4**: 1008–1017.
42. Miskin R, Zamir A, Elson D. *Biochem. Biophys. Res. Commun.* 1968; **33**: 551–557.
43. Vogel Z, Vogel T, Zamir A, Elson D. *J. Mol. Biol.* 1971; **60**: 339–346.
44. Zamir A, Miskin R, Vogel Z, Elson D. *Methods Enzymol.* 1974; **30**: 406–426.
45. Bayfield MA, Dahlberg AE, Schulmeister U, Dorner S, Barta A. *Proc. Natl. Acad. Sci. USA* 2001; **98**: 10096–10101.
46. Agrawal RK, Penczek P, Grassucci RA, Burkhardt N, Nierhaus KH, Frank J. *J. Biol. Chem.* 1999; **274**: 8723–8729.
47. Calendar R, Berg P. *J. Mol. Biol.* 1967; **26**: 39–54.
48. Briza P, Ellinger A, Winkler G, Breitenbach M. *J. Biol. Chem.* 1990; **265**: 15118–15123.
49. Cosloy SD, McFall E. *J. Bacteriol.* 1973; **114**: 685–694.
50. Soutourina J, Blanquet S, Plateau P. *J. Biol. Chem.* 2000; **275**: 11626–11630.
51. Yamane T, Miller DL, Hopfield JJ. *Biochemistry* 1981; **20**: 7059–7064.
52. Heckler TG, Roesser JR, Xu C, Chang PI, Hecht SM. *Biochemistry* 1988; **27**: 7254–7262.
53. Bain JD, Diala ES, Glabe CG, Wacker DA, Lyttle MH, Dix TA, Chamberlin AR. *Biochemistry* 1991; **30**: 5411–5421.
54. Dedkova LM, Fahmi NE, Golovine SY, Hecht SM. *J. Am. Chem. Soc.* 2003; **125**: 6616–6617.
55. Gabashvili IS, Gregory ST, Valle M, Grassucci R, Worbs M, Wahl MC, Dahlberg AE, Frank J. *Mol. Cell.* 2001; **8**: 181–188.
56. Tenson T, Ehrenberg M. *Cell* 2002; **108**: 591–594.
57. Gong F, Yanofsky C. *Science* 2002; **297**: 1864–1867.
58. Liao S, Lin J, Do H, Johnson AE. *Cell* 1997; **90**: 31–41.
59. Stroud RM, Walter P. *Curr. Opin. Struct. Biol.* 1999; **9**: 754–759.
60. Morris DR, Geballe AP. *Mol. Cell. Biol.* 2000; **20**: 8635–8642.
61. Chepkwony HK, Roets E, Hoogmartens J. *J. Chromatogr. A.* 2001; **914**: 53–58.
62. Auerbach T, Bashan A, Harms J, Schluenzen F, Zarivach R, Bartels H, Agmon I, Kessler M, Pioletti M, Franceschi F, Yonath A. *Curr. Drug Targets-Infect. Disord.* 2002; **2**: 169–186.
63. Unge J, Berg A, Al-Kharadaghi S, Nikulin A, Nikonov S, Davydova N, Nevskaya N, Garber M, Liljas A. *Structure* 1998; **6**: 1577–1586.
64. Davydova N, Streltsov V, Wilce M, Liljas A, Garber M. *J. Mol. Biol.* 2002; **322**: 635–644.
65. White O, Eisen JA, Heidelberg JF, Hickey EK, Peterson JD, Dodson RJ, Haft DH, Gwinn ML, Nelson WC, Richardson DL, Moffat KS, Qin H, Wanda Pamphile LJ, Crosby M, Shen M, Vamathevan JJ, Lam P, McDonald L, Utterback T, Zalewski C, Makarova KS, Aravind L, Daly MJ, Minton KW, Fleischmann RD, Ketchum KA, Nelson KE, Salzberg S, Smith HO, Craig J, Fraser CL. *Science* 1999; **286**: 1571–1577.
66. Levin-Zaidman S, Englander A, Shimon E, Sharma A, Minton W, Minsky A. *Science* 2003; **299**: 254–256.
67. Lu M, Steitz TA. *Proc. Natl. Acad. Sci. USA* 2000; **97**: 2023–2028.
68. Fedorov R, Meshcheryakov V, Gongadze G, Fomenkova N, Nevskaya N, Selmer M, Laurberg M, Kristensen O, Al-Karadaghi S, Liljas A, Garber M, Nikonov S. *Acta Crystallogr. D. Biol. Crystallogr.* 2001; **57**: 968–976.
69. Rheinberger HJ, Sternbach H, Nierhaus KH. *Proc. Natl. Acad. Sci. USA* 1981; **78**: 5310–5314.
70. Lill R, Wintermeyer W. *J. Mol. Biol.* 1987; **196**: 137–148.
71. Dabrowski M, Spahn CM, Schafer MA, Patzke S, Nierhaus KH. *J. Biol. Chem.* 1998; **273**: 32793–32800.
72. Noller HF, Yusupov MM, Yusupova GZ, Baucom A, Cate JH. *FEBS Lett.* 2002; **514**: 11–16.